Expanded View Figures

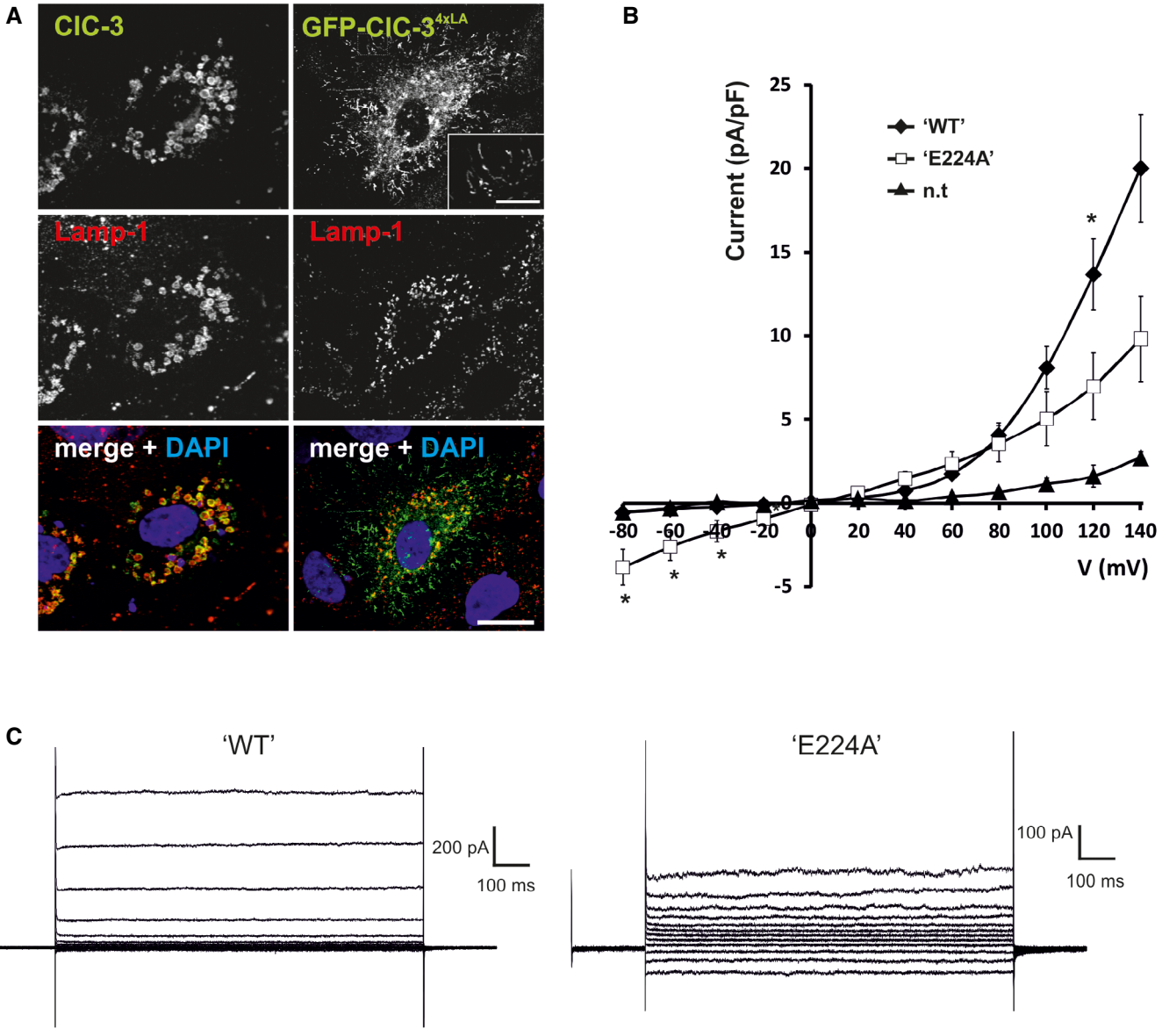

Figure EV1. Currents of partially plasma membrane directed "WT" ClC-3 and its E224A mutant.

A When transfected into HeLa cells, wild-type ClC-3 (green) localized to enlarged Lamp-1-positive (red) late endosomes/lysosomes, GFP-ClC-3^{4xLA} (green) co-localizes with Lamp-1 (red) in normal sized vesicular structures, but is also partially redirected to the plasma membrane. DNA stained with DAPI [scale bar at bottom: 20 μm (for all panels); scale bar in inset: 5 μm].

B Current–voltage relationships of HeLa cells, either non-transfected controls or transiently transfected with GFP-ClC-3^{4xLA} ("WT") and GFP-ClC-3^{4xLA} E224A ("E224A"). Cells were examined 48–72 h post-transfection by whole-cell patch-clamp using 1-s voltage pulses and 20-mV increments from −80 to +140 mV. n.t., not transfected. Mean values ± SEM "WT", n = 8; "E224A", n = 4; n.t., n = 4, *P < 0.05, MW test. Currents of surface-directed GFP-ClC-3^{4xLA} were strongly outwardly rectifying and similar to ClC-3 currents reported by others (Li *et al*, 2002; Picollo & Pusch, 2005; Matsuda *et al*, 2008; Guzman *et al*, 2013) and as described for a ClC-5/ClC-3 chimera (Rohrbough *et al*, 2018). They resembled currents of ClC-4 and ClC-5 (Steinmeyer *et al*, 1995; Friedrich *et al*, 1999) but were only barely above background. Mutating the "gating glutamate" E224 to alanine abolished rectification, as reported for ClC-3 (Li *et al*, 2002; Matsuda *et al*, 2008; Rohrbough *et al*, 2018), ClC-4, and ClC-5 (Friedrich *et al*, 1999) and ClC-7 (Leisle *et al*, 2011). These low expression levels precluded measurements of H^+-transport, but recent studies using ClC-5/3 chimeras convincingly demonstrate that ClC-3 is a Cl^-/H^+-antiporter which can be uncoupled by the E224A ("unc") mutation (Rohrbough *et al*, 2018).

C Example traces of GFP-ClC-3^{4xLA} ("WT") and GFP-ClC-3^{4xLA} E224A ("E224A").

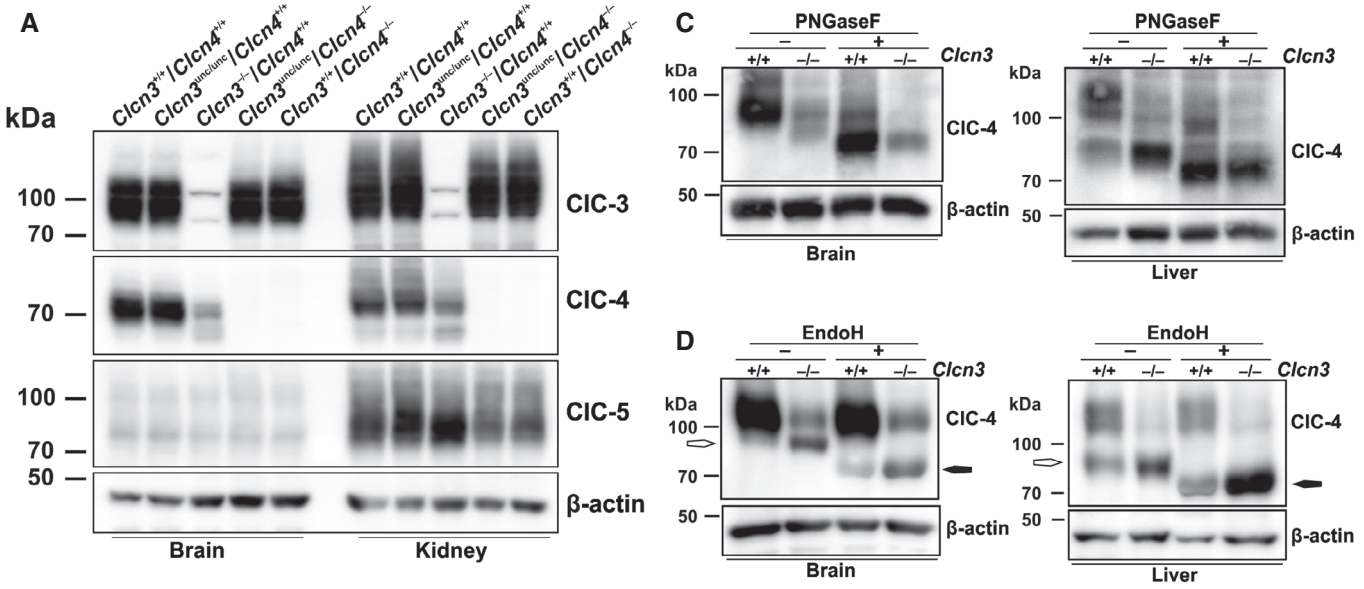

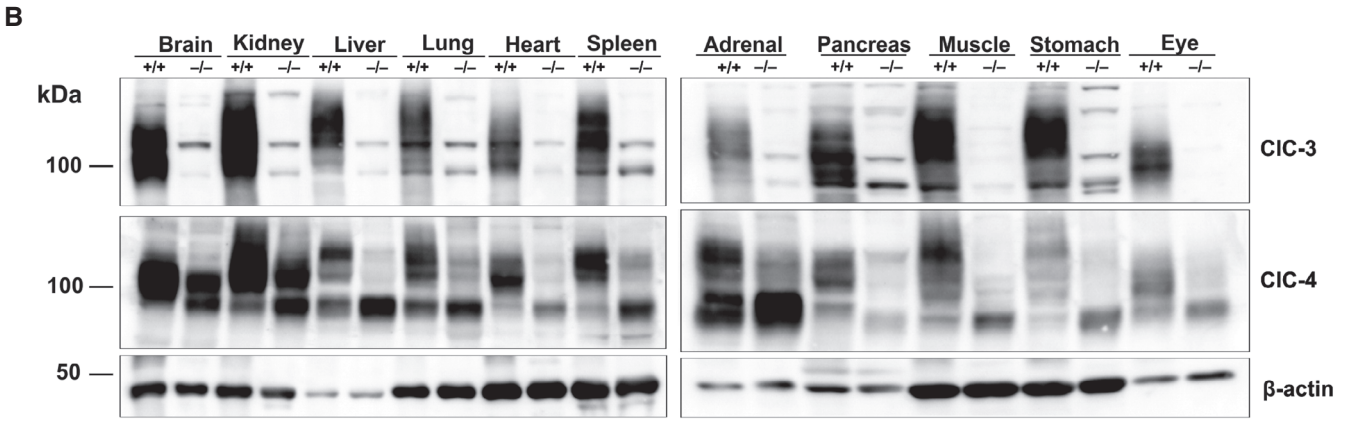

Figure EV2. Effect of ClC-3 on ClC-4 levels and glycosylation in various tissues.

A Western blots for ClC-3, ClC-4, and ClC-5 of membrane fractions isolated from brain and kidney from mice of the indicated genotypes. Whereas ClC-4 protein levels depend on ClC-3, ClC-3 levels do not depend on ClC-4. β-Actin served as a loading control.

B Immunoblots for ClC-3 and ClC-4 of membrane fractions isolated from indicated organs of WT and *Clcn3*$^{-/-}$ mice (indicated by +/+ and −/−). β-Actin, loading control. The different sizes of ClC-4-positive bands most likely result from differences in glycosylation between tissues. Disruption of ClC-3 leads to the appearance, or increase in intensity, of the lowest band that represents the immature protein. The ratio between ClC-3 and ClC-4 proteins apparently differs between tissues.

C Effect of PNGase F on ClC-4 in brain and liver membrane fractions of WT (+/+) and *Clcn3*$^{-/-}$ (−/−) mice. Removal of N-linked glycans by PNGase F reveals that apparent size differences of ClC-4 between WT and *Clcn3*$^{-/-}$ tissues are owed to less glycosylation of ClC-4 in the absence of ClC-3.

D Treatment of brain and liver membranes with EndoH reveals that a large portion of ClC-4 in *Clcn3*$^{-/-}$ tissue has not left the ER. The arrows are pointing to the fractions of ClC-4 protein that are sensitive to endoglycosidase H treatment, i.e., has not been modified in the Golgi.

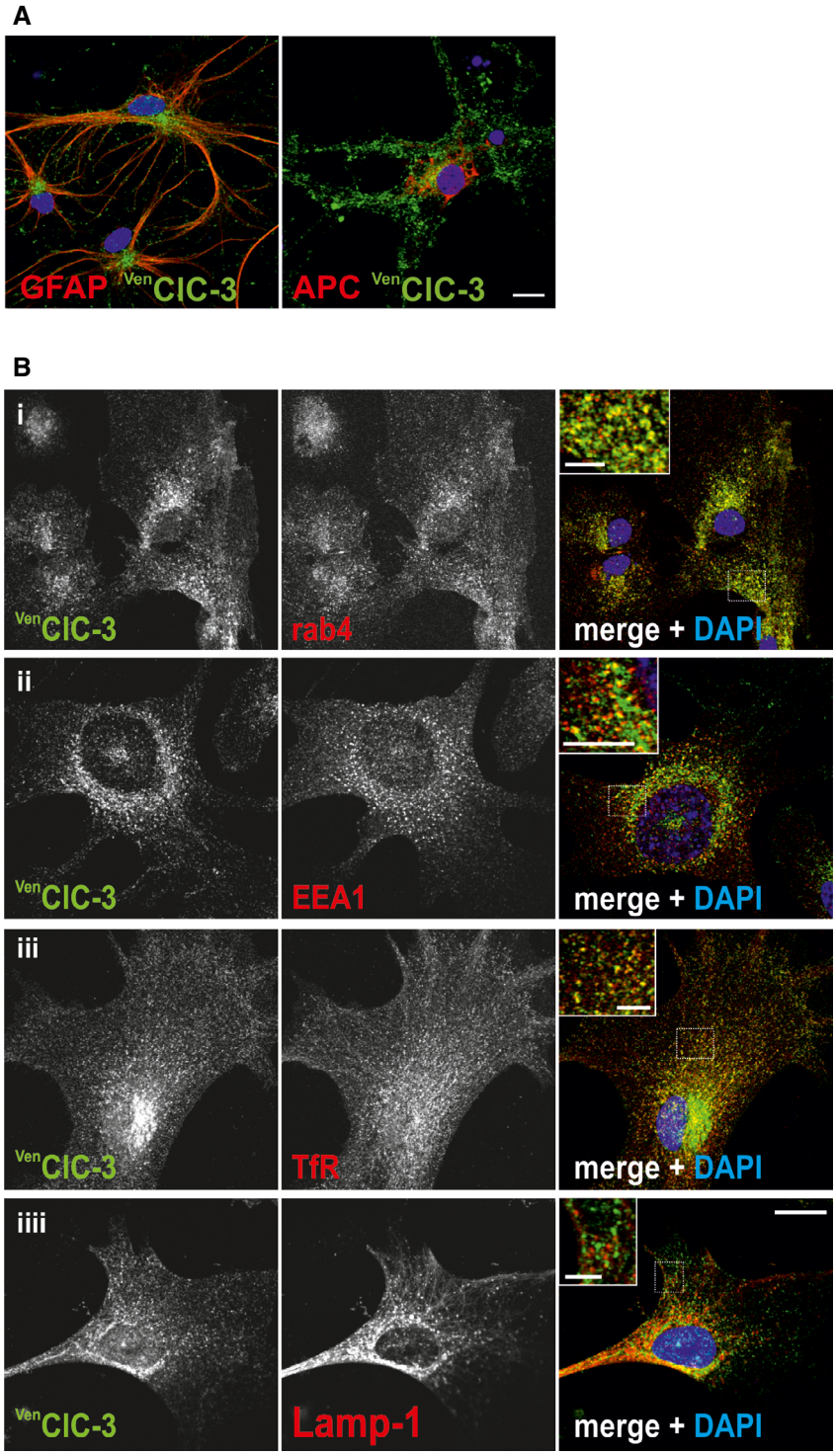

Figure EV3. Expression and subcellular localization of ^{Venus}ClC-3 in cultured glial cells.

A Primary cultured glial cells were labeled for ^{Venus}ClC-3 (green) and GFAP or APC (red, left and right panel, respectively), markers for astrocytes and oligodendrocytes, respectively (scale bar: 10 μm for main panels; scale bar in insets: 5 μm).

B Primary cultured astrocytes were labeled for ^{Venus}ClC-3 (green) and rab4 (i, red), EEA1 (ii, red), TfR (iii, red), and Lamp-1 (iv, red) (scale bars: 20 μm in i, iii, and iv; 10 μm in ii). The inlays depict magnified views of boxed sections. DNA stained with DAPI.

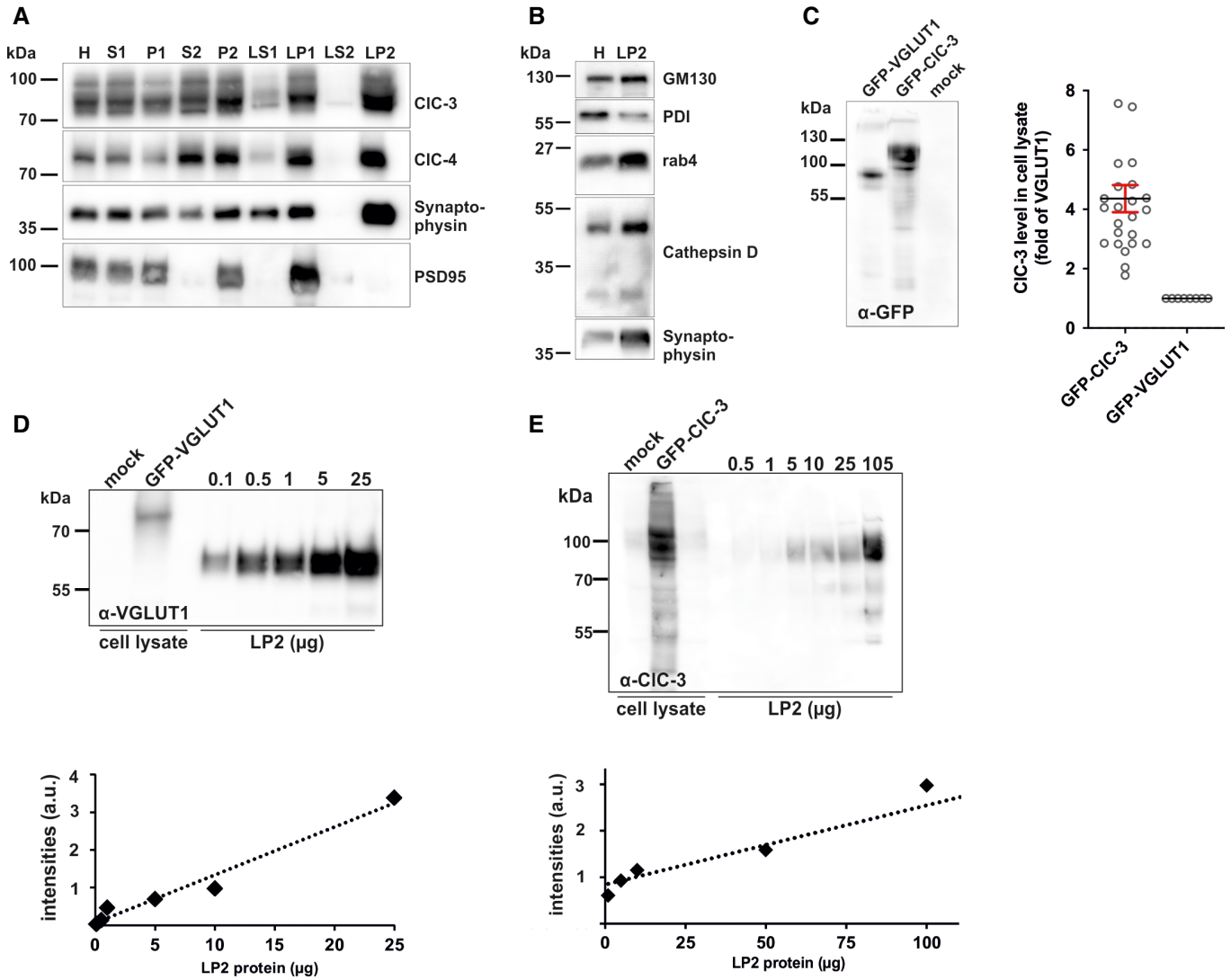

Figure EV4. Characterization and quantification of ClC-3 in LP2 fraction.

A, B Characterization of SV-enriched LP2 fraction. (A) Western blots for ClC-3, ClC-4, synaptophysin, and PSD95 (postsynaptic marker) of fractions obtained during synaptic vesicle-enriched fraction (LP2) preparation using differential centrifugation as described (Huttner *et al*, 1983; Takamori *et al*, 2000). (B) Immunoblots for different cellular markers comparing whole lysate (H) and synaptic vesicle-enriched fraction (LP2) (GM130, Golgi marker; PDI, ER marker; rab4, early endosomes and SV; cathepsin D, lysosomal marker; synaptophysin, SV marker).

C–E Quantification of ClC-3 in LP2 fractions (C) Western blot of lysates from HEK cells transiently overexpressing either mVGLUT1 or hClC-3, which were both fused at their N terminus to GFP. Probing for the GFP tag allows to directly compare the relative amount of ClC-3 and VGLUT1 in the lysate for its use as calibration standards for anti-ClC-3 and anti-VGLUT1 antibodies in Western blots of tissue standards [as in (D) and (E)]. (n = 3 independent transfections, horizontal lines and error bars represent mean values SEM). The standard contains about 4.33 × more ClC-3 molecules than the standard for VGLUT1. (D) Example immunoblot for VGLUT1 in which the GFP-VGLUT1 standard [same lysate as in (A)] is compared to different amounts of LP2 fraction. Below, example plot in which WB signals are plotted against rising amounts of the LP2 fraction, quantified by protein contents. The standard for VGLUT1 roughly corresponds to 2.5 µg of LP2 fraction (averaged from n = 6 Western blots). (E) Same as shown in (D) but for ClC-3. The standard for ClC-3 roughly corresponds to 140 µg of the LP2 fraction (n = 7). From (A) and (B), we calculated a molecular ratio for ClC-3/VGLUT1 ≈ 2.5/(140*4.33) = 4.12×10^{-3} = 1/243 in our LP2 fraction. Considering that ClC-3 may form not only hetero- but also homodimers and that SVs are ~ 2-fold enriched in the SV compared to the LP2 fraction (Huttner *et al*, 1983) and that there are ~ 10 copies of VGLUT1 per vesicle (Takamori *et al*, 2006), our data yield an upper limit of one ClC-3-containing transporter on roughly every 25th SV. This upper limit assumes that in LP2 fractions ClC-3 is only present on SVs. Any contamination with other ClC-3-containing compartments like endosomes, as found in this work, will lower this estimate. The ~ 20-fold lower value for the ClC-3/VGLUT1 ratio given by (Schenck *et al*, 2009) may have been caused by their calibration of the VGLUT1 antibody (Synaptic Systems) that recognizes an epitope at the C terminus of VGLUT1. It might have been shielded by the GFP, which these authors fused directly to the carboxy terminus of VGLUT1, thereby overestimating the number of VGLUT1 molecules in their preparation (S. Takamori, *personal communication*).

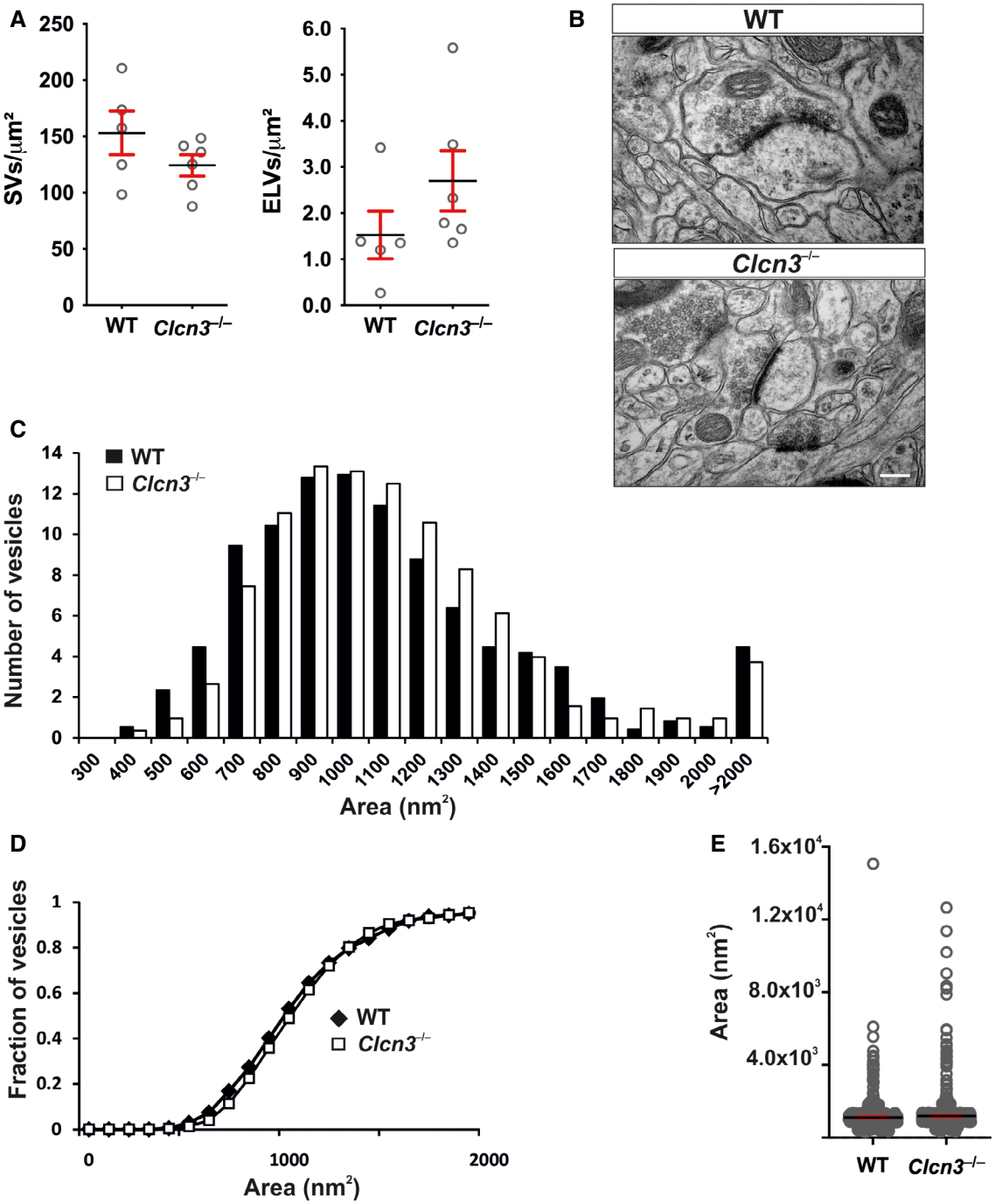

Figure EV5. ***Clcn3*$^{-/-}$ mice display normal synaptic ultrastructure.**

A Quantification of SVs and endosome-like vacuoles (ELVs) of glutamatergic spine synapses from layer 4–5 of secondary visual cortex of P14, P21, and P70 days-old *Clcn3*$^{+/+}$ and *Clcn3*$^{-/-}$ animals. Mean ± SEM is shown. Five animals per genotype, 20–25 boutons/animal.

B Example electron micrographs illustrating normal morphology of the pre- and postsynapse of *Clcn3*$^{+/+}$ and *Clcn3*$^{-/-}$ mice (scale bar: 250 nm).

C Histogram indicating the distribution of synaptic vesicles sizes of *Clcn3*$^{+/+}$ and *Clcn3*$^{-/-}$ mice. Five animals per genotype, around 150 vesicles/animal.

D Cumulative plot represents the SV size distribution in *Clcn3*$^{+/+}$ and *Clcn3*$^{-/-}$ mice. Five animals per genotype, around 150 vesicles/animal.

E Mean area of all vesicles is unchanged between *Clcn3*$^{+/+}$ and *Clcn3*$^{-/-}$ mice. Mean ± SEM is shown. Five animals per genotype, around 150 vesicles/animal.